Cold Regions Science and Technology 148 (2018) 38–49

Contents lists available at ScienceDirect

Cold Regions Science and Technology

journal homepage: www.elsevier.com/locate/coldregions

Ground-penetrating radar studies of permafrost, periglacial, and near-surface geology at McMurdo Station, Antarctica

Seth Campbell[a,b,c,*], Rosa T. Affleck[a], Samantha Sinclair[a]

[a] Engineer Research and Development Center, Cold Regions Research and Engineering Laboratory (ERDC-CRREL), Hanover, NH, USA
[b] University of Maine, School of Earth and Climate Sciences, Orono, ME, USA
[c] University of Washington, Quaternary Research Center and the Department of Earth and Space Sciences, Seattle, WA, USA

ARTICLE INFO

Keywords:
Ground-penetrating radar
Excess ice
Permafrost
Ice-rich fill
Fractured volcanic bedrock

ABSTRACT

Installations built on ice, permafrost, or seasonal frozen ground require careful design to avoid melting issues. Therefore, efforts to rebuild McMurdo Station, Antarctica, to improve operational efficiency and consolidate energy resources require knowledge of near-surface geology. Both 200 and 400 MHz ground-penetrating radar (GPR) data were collected in McMurdo during January, October, and November of 2015 to detect the active layer, permafrost, excess ice, fill thickness, solid bedrock depth, and buried utilities or construction and waste debris. Our goal was to ultimately improve surficial geology knowledge from a geotechnical perspective. Radar penetration ranged between approximately 3 and 10 m depth for the 400 and 200 MHz antennas, respectively. Both antennas successfully detect buried utilities and near-surface stratified material to ~0.5–3.0 m whereas 200 MHz profiles were more useful for mapping deeper stratified and un-stratified fill over bedrock. Artificially generated excess ice which appears to have been created from runoff, water pooling and refreezing, aspect shading from buildings, and snowpack buried under fill, are prevalent. Results show that McMurdo Station has a complex myriad of ice-rich fill, scoria, fractured volcanic bedrock, permafrost, excess ice, and buried anthropogenically generated debris, each of which must be considered during future construction.

1. Introduction

McMurdo Station, located on Hut Point Peninsula of Ross Island, was first used as a shoreline base in 1902 to explore inland Antarctica (Fig. 1). The United States more permanently established a base beginning in the mid-1950s to support Antarctic research (Sullivan, 1957). Relatively rapid expansion occurred through the 1960s and 1970s (Klein et al., 2008a, 2008b), resulting in McMurdo now acting as the logistics hub for research, managed by the U.S. Antarctic Program (USAP). The station has been altered to accommodate increasing science activities (Klein et al., 2008a; Klein et al., 2008b; Kennicutt et al., 2010) over the past several decades, primarily through filling of bedrock voids to flatten terrain and the installation of dirt pads or platforms for buildings. Natural geomorphological features have therefore been destroyed or covered over at the surface within McMurdo Station (Cole et al., 1971; Crockett, 1998; Klein et al., 2008a, 2008b; Klein et al., 2012; Kennicutt II et al., 2010). However, moraines, permafrost polygons, massive ice wedges, and other shallow geomorphology features are still visible at the station borders, suggesting their prior existence also on station grounds. Secondary impacts from McMurdo activities include increased airborne dust from vehicle traffic, which has altered snowpack albedo; associated melt water runoff from local snowfields; a deepening of the active layer or complete thawing of permafrost; and increased stream flow and erosion (Campbell et al., 1994; Klein et al., 2008a, 2008b; Affleck et al., 2012, 2014a, 2014b; and Affleck and Carr, 2015). Accidental or historical human activity, such as chemical spills, fuel leaks, garbage and construction debris burial, is also prevalent at McMurdo Station, resulting in increased subsurface complexity relative to other similar near-surface geology study sites. The slow biological degradation of pollutants within polar environments allows them to persist and accumulate over long periods of time or to last indefinitely. Water runoff during warmer months can flush or redistribute these pollutants resulting in uncertainties of their fate and transport (Affleck et al., 2014c).

Ultimately, USAP has a master plan to modernize, update, or replace existing facilities with interconnected, environmentally sustainable, and energy-efficient facilities on the existing footprint. This master plan will require significant site preparation, and a critical piece of this effort is a geological analysis of McMurdo to incorporate into geotechnical decisions related to structural planning and design.

* Corresponding author at: 72 Lyme Rd., Hanover, NH 03755, USA.
E-mail address: scampb64@umaine.edu (S. Campbell).

https://doi.org/10.1016/j.coldregions.2017.12.008
Received 29 November 2016; Received in revised form 16 December 2017; Accepted 18 December 2017
Available online 24 December 2017

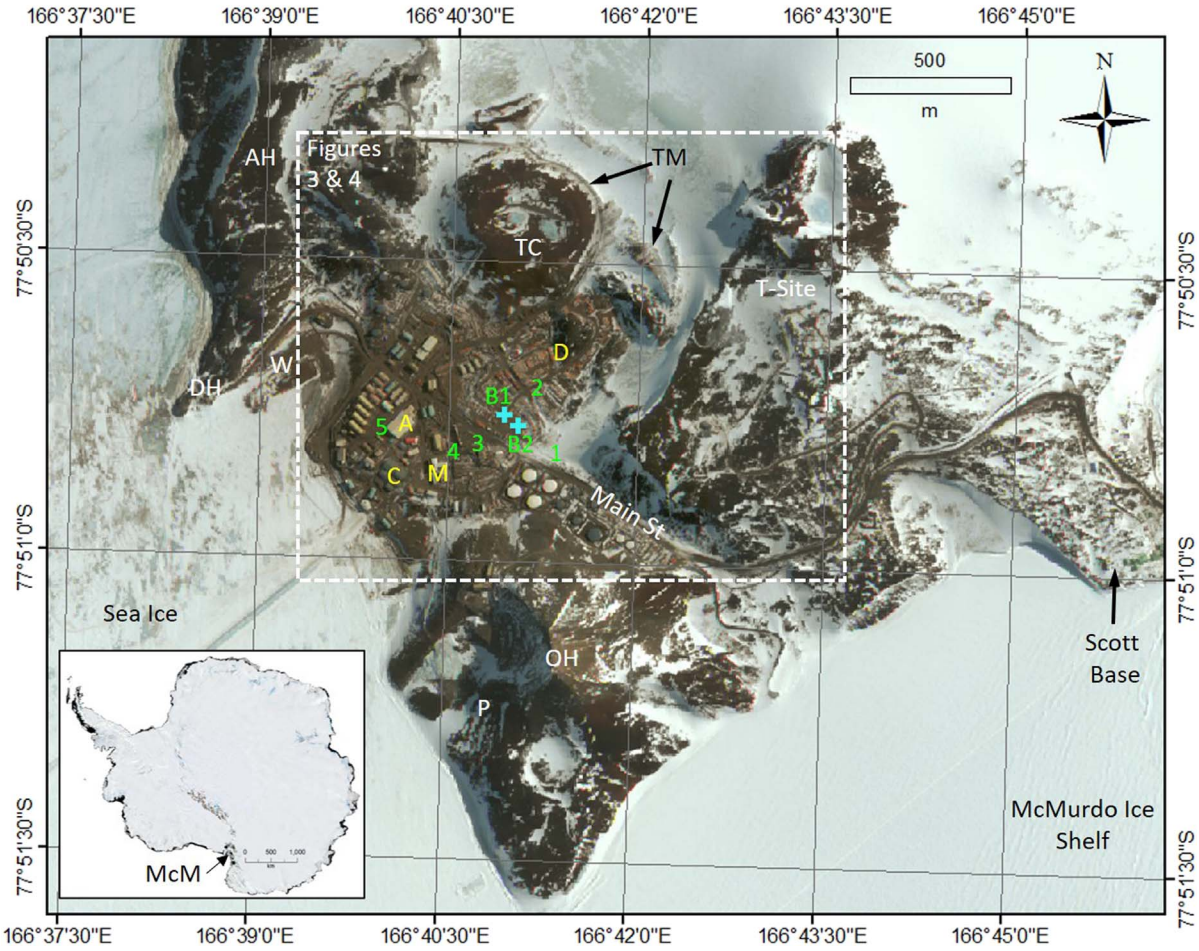

Fig. 1. Map of McMurdo Station on Ross Island, Antarctica showing major geographic features Labels include Observation Hill (OH), Discovery Hut (DH), terminal moraines (TM) north of McMurdo Station (McM), permafrost polygons (P), Arrival Heights (AH), Winter Quarters Bay (W), Twin Craters (TC), T-Site, the dump (D), Building 155 (A), Crary Lab (C), Mechanical Equipment Center (M), referenced borehole locations (B1 and B2 with + symbols), and excavated pits (1 through 5). The white dashed box outlines the location of more detailed Figs. 3 and 4.

Although significant mineralogy, petrology, and soil analyses have been conducted on Hut Point Peninsula (e.g., Cole et al., 1971; Kyle and Muncy, 1989; Wright et al., 1982), ours is the first geophysical survey of its kind that we are aware of to study both the natural near-surface geology and the anthropogenic influences on geomorphology of McMurdo Station. The objectives of this study are to therefore (1) identify permafrost and excess ice within perennially frozen sediments; (2) characterize extent and thickness of stratified or unstratified till over bedrock; (3) estimate moisture variability; (4) differentiate between anthropogenic and natural fill material; (5) locate buried utilities, conduits, debris or other anthropogenic structures that would have implications for long-term infrastructure planning; and (6) develop recommendations for broader-scale geotechnical planning based on the near-surface geology and geomorphology determined from geophysics.

2. McMurdo Station geology and geomorphology

The geology of Hut Point Peninsula near McMurdo Station primarily consists of olivine basalt, hornblende trachyte, and hornblende basalt. Autoclastic and pyroclastic breccias are exposed on the surface just north of McMurdo Station, suggesting that their existence is possible within the near subsurface at McMurdo (Cole et al., 1971). Rock ages range between 0.5 and 2 million years, relatively young compared to the surrounding region, which displays volcanic rocks dating back 18 million years (Kyle and Muncy, 1989). From a historical context, prior glaciation of Hut Point Peninsula has deposited tills across McMurdo valley and a terminal moraine exists immediately north of McMurdo Station (Fig. 1), suggesting that the primary retreating glacier of this region has been stalled long enough during the recent past to generate such a feature. The till mainly consists of the host local volcanic material, namely heavily weathered, fractured, and unsorted basalt and scoria that is ice-rich within its pores and interstitial spaces. Permafrost and classic structures that are indicative of massive ice, such as permafrost polygons, also surround McMurdo Station in regions unaltered by human activity, such as immediately south of Observation Hill (Fig. 1). The near-surface soils experience diurnal or seasonal temperature fluctuations, resulting in thawing or freezing of the active layer, which consists both of natural till and anthropogenically altered or placed fill during McMurdo construction operations (Affleck et al., 2017). Shallow (3 m) boreholes (Fenwick and Winkler, 2016) show relatively high percent ice volumes of greater than 20% from either buried snow or refreezing meltwater across McMurdo, and shallow pits excavated in conjunction with this project revealed high gravimetric water content, between 64% and 150% at 0.5–1.0 m depth (Affleck et al., 2017; Fig. 2). These results suggest that any geotechnical engineering must consider potential thaw impacts across McMurdo. Unfortunately, boreholes and pits represent point measurements of the subsurface and have limited applicability without some knowledge of lateral continuity of structures outside of the borehole or pit sites. The incorporation of geophysical data can provide a pseudo-three-dimensional picture of the near surface. However, like boreholes and pits,

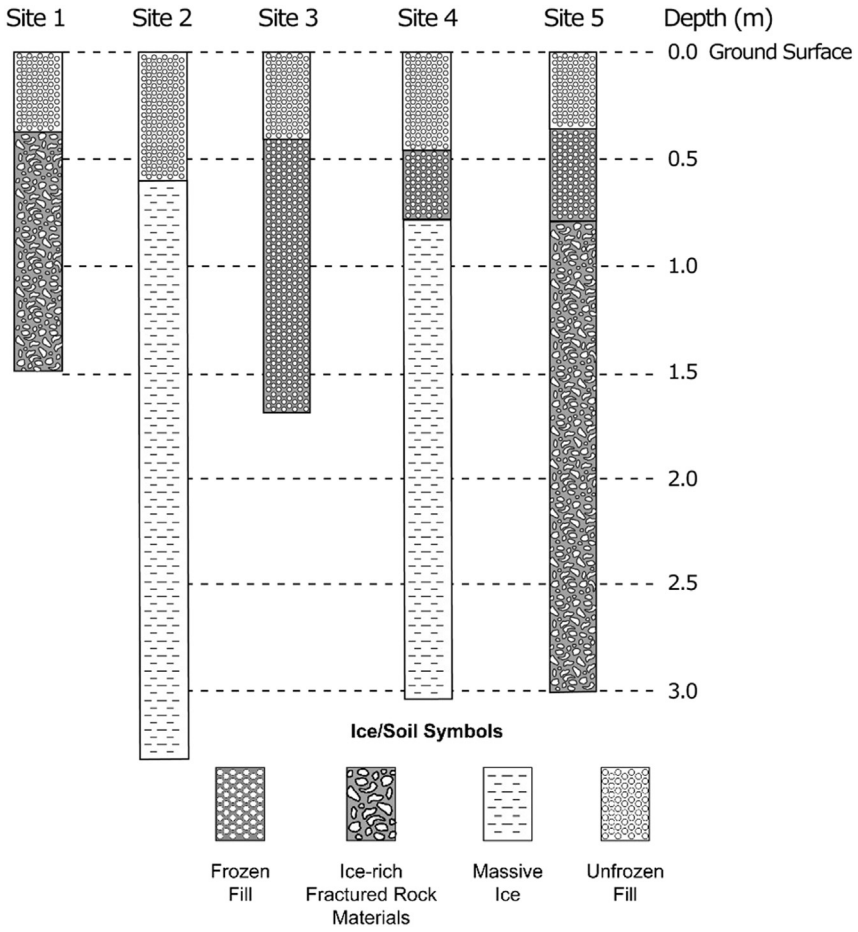

Fig. 2. Pit logs from Affleck et al. (2017) that were extracted in the winter of 2015–2016, which were used as ground truth for GPR profiles at McMurdo Station.

geophysics can provide only limited information on subsurface structure because numerous assumptions are required without some form of ground truth. This results in a consistent challenge, which combined ground-truth and geophysical methods are particularly well suited for solving. Below, we outline the most significant benefits and limitations of this coupled effort in a complex polar environment.

3. Methods

Ground-penetrating radar (GPR) data was collected in January, November, and December of 2015 on and off roads and trails covering both disturbed and undisturbed surfaces. We used a SIR-4000 GPR control unit coupled with model 5,106,200 MHz and model 50,400 400 MHz shielded antennas, each unit manufactured by Geophysical Survey Systems Incorporated (GSSI). The GPR was synced with a Trimble 5700 and Zephyr geodetic antenna that recorded GPS locations at a frequency of 1 Hz. GPR scans were recorded at 24 scans s^{-1}, and antennas were towed by hand on plastic sleds at approximately 0.5 m s^{-1}, resulting in traces being recorded approximately every 2 cm in horizontal distance. GPR profiles were collected using a real-time kinematic (RTK) radio that transmitted at 418 MHz for 200 MHz profiles, resulting in 1–10 cm surface precision of profiles. The 400 MHz profiles were collected without a RTK system because, despite the antenna being shielded, the GPS radio still interfered with the data, and we were unable to filter the radio signal without significantly degrading the data of interest. Therefore, the 400 MHz data accuracy is estimated to have spatial uncertainty between 1 and 3 m. Scans were recorded for 150–250 ns TWTT (two-way travel time) with 1024 samples per scan, resulting in about 4 samples ns^{-1}. Given that the relative permittivity ($\dot{\varepsilon}$) in volcanic rock for McMurdo Station ranges between 6 and 12 (explanation below), which has associated wave velocities of 0.122–0.087 m ns^{-1} for lower to higher values of $\dot{\varepsilon}$, respectively, 50–60 samples m^{-1} were recorded vertically. This vertical sample resolution is more than sufficient to maintain a smooth waveform given the frequencies used. Range gain, high- and low-pass finite impulse response (FIR) filtering between 100 and 800 MHz were both applied during data collection. Profiles were post-processed using GSSI Radan Version 7.0 proprietary software. Post processing included time-zero correction, integration of GPS data into the files, horizontal filtering to remove ringing and the direct wave within the data, and stacking to improve signal-to-noise ratios and visualization of horizontal reflectors. GPS locations were interpolated between the duration of each GPS measurement using Radan. We used the same software to map the thickness of stratified material (Fig. 3) depth to bedrock (Fig. 4), and finite targets of interest, including areas of excess ice and buried utilities.

4. Interpretation methods and assumptions

Depth calibration was performed by using pits excavated for this study (Affleck et al., 2017; Fig. 2), borehole logs from November to December 2015 (Fenwick and Winkler, 2016), geophysical observations of the subsurface in relation to pit and core observations, and via variable velocity migration of GPR profiles. For example, we linked stratigraphic thicknesses, apparent dip, orientations, and continuity of major horizons in pits (which were typically 2–12 m long) to similar geometrical observations within GPR profiles. Each pit displayed some lateral variability of layer thicknesses, so pit interpretations (Fig. 2) represent average unit thicknesses. Pits and cores were generally located 1–2 m from GPR profiles, providing reasonable accuracy of

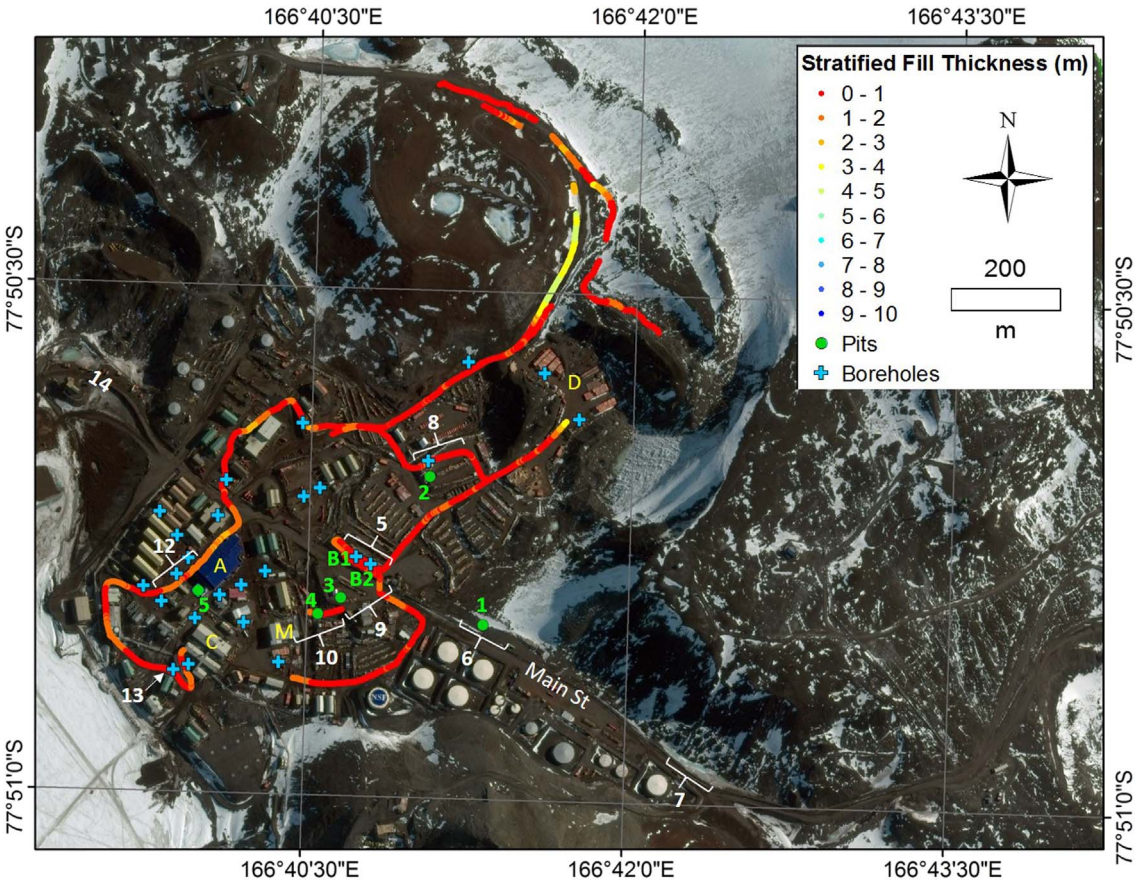

Fig. 3. Map of GPR profiles showing interpreted stratified fill thicknesses over McMurdo Station. Note thicknesses generally increase near the shoreline of McMurdo and decrease towards the northeast. Green numbers correspond to numbered pits (1 thru 5) and core sites (B1 and B2), white numbers correspond to radar figures (Figs. 5–14), and yellow letters correspond to Building 155 (A), Crary Lab (C), dump (D), and the Mechanical Equipment Center (M). Numerous exposed outcrops in these regions confirm these geophysical interpretations. (For interpretation of the references to colour in this figure legend, the reader is referred to the web version of this article.)

structure and stratigraphic thicknesses. However, we assume some uncertainty in depth calculations because the datasets were not collected simultaneously, lateral differences exist in unit thicknesses, and there is some ambiguity in pit and core locations relative to GPR profiles.

We used typical $\acute{\epsilon}$ values for permafrost (5.3), basalt (6–12), fill (6–12), and ice (3) to determine expected geophysical responses at interfaces between geological structures (Heggy, 2012; Elshafie and Heggy, 2013; Rust et al., 1999). Waveform polarity of the first three half cycles results from an interface between two materials that have $\acute{\epsilon}$ contrasts. When a positive (+ − +) triplet occurs, it suggests that the deeper layer has a higher $\acute{\epsilon}$; and when a negative (− + −) triplet occurs, it suggests that the deeper layer has a lower $\acute{\epsilon}$, each relative to the shallower layer. For example, ice buried below frozen till would display a negative triplet response because of the transition from higher to lower $\acute{\epsilon}$. Recognizing that there is some overlap of $\acute{\epsilon}$ values between different geological materials, we incorporated migration and diffraction analyses of GPR profiles to confirm or provide ranges for $\acute{\epsilon}$ and therefore associated wave velocities and depths of features imaged using GPR. Surface diffractions and migrations estimated values of $\acute{\epsilon}$ between 6 and 12, which is consistent with erosion-resistant basalts (Heggy, 2012; Elshafie and Heggy, 2013). These assumptions were used to calculate depth of features in areas where GPR profiles were collected but ground-truth information was not available, based on the following equations:

$$V = \frac{c}{\sqrt{\acute{\epsilon}}}, \quad (1)$$

$$d = \frac{(TWTT * V)}{2}, \quad (2)$$

where V is velocity (m ns^{-1}), c is the speed of light, d is depth (m), and TWTT is two-way travel time (ns). All GPR figures show approximate values of $\acute{\epsilon}$ used for total depth calculations, based on either ground-truth from cores and pits, or migration.

Following the geophysical and ground-truth assumptions above, we also applied geomorphological and geological knowledge of near-surface structures to our GPR interpretations. For example, we assumed that horizontal and relatively continuous horizons were anthropogenically altered and layered fill or stratified fine grain materials deposited from summer water runoff. In contrast, regions that exhibited unstratified or discontinuous horizons and numerous diffractions or hyperbolas were interpreted as buried till, dumped and unsorted debris, or heavily fractured and weathered bedrock. These assumptions were based on the expected physical responses from GPR in till and bedrock environments (e.g., Arcone et al., 2014). Because of the heavily fractured and variable or rough exposed bedrock surfaces surrounding McMurdo, we developed a strategy to interpret bedrock horizons under stratified or unstratified material through two primarily assumptions. First, we assumed that consistent terminations of stratified till against an unconformity was likely a bedrock contact. Second, the interface between fill and bedrock often consisted of discrete but multiple hyperbolas that created a relatively continuous horizon, suggesting a rough but definitive surface between the overburden matrix relative to material below. Multiple ground-truth points where bedrock outcrops occur at or near the surface in McMurdo support our interpretation that these geophysical signatures likely do represent a fill and bedrock contact. Finally, GPR profiles over surface-exposed bedrock revealed

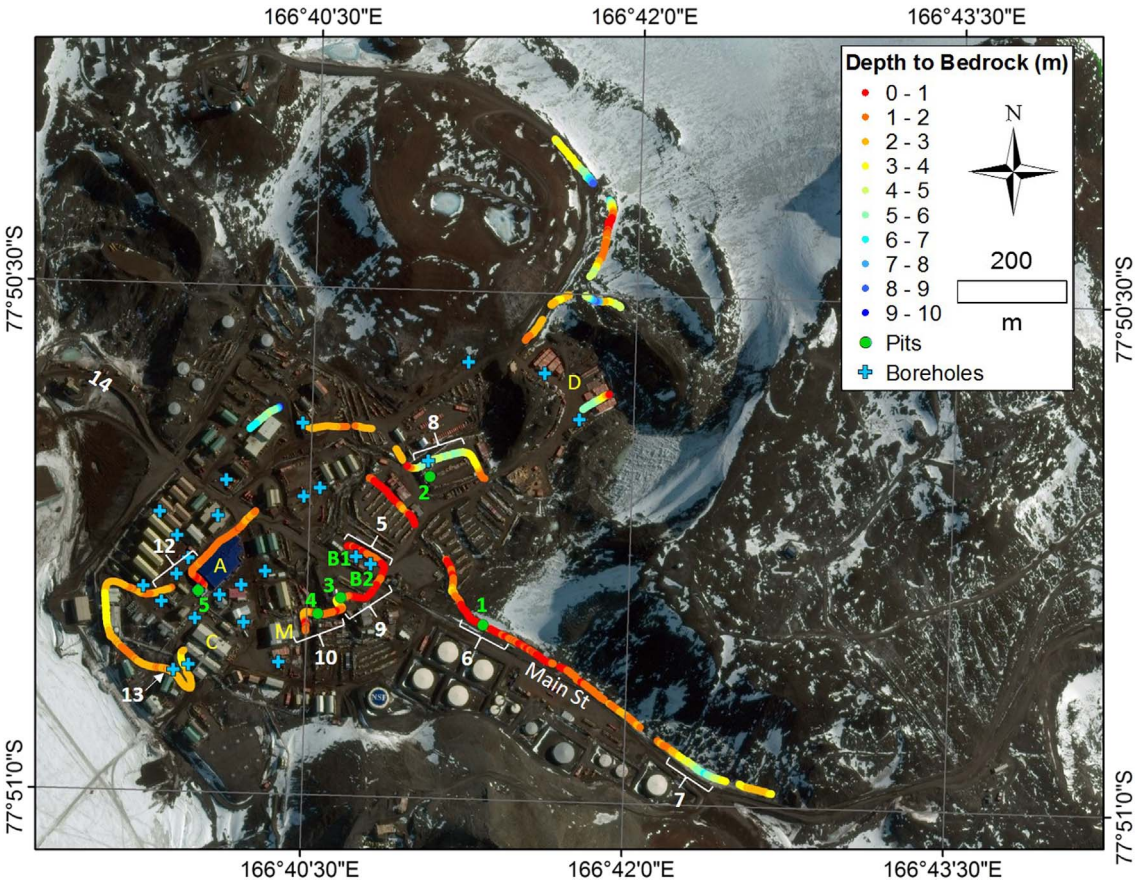

Fig. 4. Map showing interpreted depth to bedrock at McMurdo Station. Note that both the 400 and 200 MHz antennas used in this study were unable to resolve bedrock depth in much of the southern region of McMurdo near the sea ice likely due to increased thickness of fill and greater bedrock depths. Green numbers correspond to numbered pits (1 thru 5) and core sites (B1 and B2), white numbers correspond to radar figures (Figs. 5–14), and yellow letters correspond to Building 155 (A), Crary Lab (C), dump (D), and the Mechanical Equipment Center (M). (For interpretation of the references to colour in this figure legend, the reader is referred to the web version of this article.)

high attenuation rates, suggesting that below a fill-bedrock horizon, signal penetration would significantly diminish. Therefore, in some cases, we used a combination of the horizon triplet response, diffractions, and high attenuation below the horizon as grounds for bedrock interpretations.

The interpretation scheme above results in a classification that distinguishes between stratified fill (such as road fill), unstratified material (such as naturally deposited till or heavily fractured bedrock), and structurally sound bedrock. We note that in most cases, bedrock interpretations have a greater uncertainty in terms of depth and actual interpretation relative to stratified and unstratified fill. This is because most ground truth does not extend to bedrock depth, the depth of bedrock is near the maximum depth of penetration for either GPR antenna frequency, and the depth of bedrock integrates errors associated with average wave velocities dependent on a locally variable $\acute{\epsilon}$ for the material above.

5. Pits and GPR comparisons

Here we compare results from two extracted borehole cores and five excavated pits in December of 2015 to GPR profiles collected over and extending from each site.

5.1. Boreholes

Immediately north of Main Street in the McMurdo Open Storage area, Fenwick and Winkler (2016) extracted two geological cores (Figs. 1, 3, 4, and 5; B1 and B2) 30 m apart from each other as part of a drilling effort to study McMurdo near-surface geology. The cores revealed stratified and ice-rich sand and gravel in the top 0.7 to 1.2 m with the depth of fill increasing west to east (B1 to B2). Below this well-graded fill, ice-rich and unstratified fill, fractured scoria, and ultimately solid bedrock existed in the cores. We collected a corresponding 200 MHz profile over the two boreholes nearly coincident with the drilling (Fig. 5). The GPR profile reveals a relatively continuous horizon at 11–20 ns TWTT, which we interpret as the transition from the stratified and ice-rich sands and gravel to the unstratified fill, weathered and fractured bedrock, below. The TWTT to this transition corresponds with a $\acute{\epsilon}$ of ~6, which is reasonable for dry or ice-rich sand and gravel.

5.2. Site 1

A 200 MHz GPR profile collected near pit 1 was 930 m long and oriented parallel to Main Street. The profile originated near the top of a fill pad situated north of Main Street and traversed to the valley between Observation Hill and T-Site Hill (Figs. 1, 3, 4 and 6). The sole ground-truth pit extracted along this entire transect reveals a 0.35 to 0.5 m thick overburden of stratified fill with the top 0.3 m generally being thawed and the bottom 0.2 m being frozen (Fig. 2). Below the fill, a generally poorly sorted and ice-rich fractured rock matrix exists. The corresponding GPR profile (Fig. 6) reveals two subparallel and continuous horizons between 0.3 and 0.5 m ($\acute{\epsilon}$ = 8), the lower of which we interpret to be a transition between the overburden to ice-rich fractured rock matrix. The parallel horizons we interpret to be stratified fill that has been worked by heavy equipment during construction operations. Few reflections below this horizon were visible along the length of the GPR profile. We suggest that solid bedrock is likely deeper than we could image over the fill pad. However, further to the east, the profile

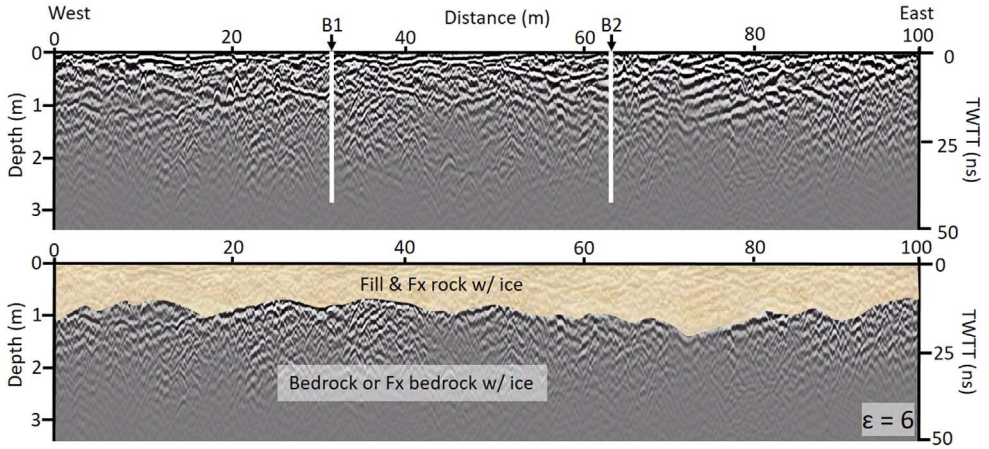

Fig. 5. 200 MHz GPR profile (top) with interpretation (bottom) showing stratified fill and fractured ice-rich rock situated over bedrock.

significantly improves (Fig. 7), and multiple continuous horizons become evident. We interpret these multiple horizons to be excess or massive ice residing over multiple layers of ice-rich fill and eventually heavily fractured ice-rich bedrock between 5 and 7 m depth.

5.3. Site 2

At site 2, a core and pit from the same location were both used for comparison to GPR profiles (Fig. 2). The site is located on a raised sediment platform towards the northern region of McMurdo Station. Both the core and pit revealed dipping and stratified sediment within a predominantly ice-rich matrix to 2.21 m and 3.35 m, respectively. A 200 MHz GPR profile across the pit and borehole reveal two major dipping horizons, suggesting progressive decreases in $\acute{\epsilon}$ values with depth to a horizon at 100 ns TWTT (Fig. 8; black arrows in top panel). At that depth, the dipping horizons are truncated by another parallel horizon; that interface suggests an increase in $\acute{\epsilon}$ at greater depths. We interpret the two internal horizons as sediment-rich layers within ice which was created from sediments being deposited over snow during construction of the platform. This interpretation is consistent with core and pit observations. The deepest horizon at 100 ns is interpreted as bedrock, based on the increase in $\acute{\epsilon}$, the unconformity relative to the dipping stratigraphy above, and known shallow bedrock surrounding this raised platform. However, ground truth does not reach this depth for absolute confirmation of the interpretation.

5.4. Site 3

At site 3, a pit was excavated on the southern side of Main Street (Fig. 2) near a steep slope above the Mechanical Equipment Center (Fig. 1; M). A corresponding 200 MHz profile (Fig. 9) was collected across the pit extraction site and traversed approximately northeast to southwest across and perpendicular to Main Street. The pit was excavated to a 1.6 m depth and revealed shallow stratified and unfrozen fill for the top 0.4 m and frozen stratified fill over permafrost down to the maximum pit depth. Fill consisted of significant amounts of construction debris and a hydrocarbon odor consistent with other pits and cores from 2015 and 2016 (Fenwick and Winkler, 2016; Affleck et al., 2017). The 200 MHz profile collected in this region crossed bedrock exposed on Main Street, which acted as an excellent ground-truth point for the rest of the profiles collected in this area due to its easily traceable horizon beneath fill laterally from the surface outcrop. Stratification of fill was visible where the profile crossed the pit location, and bedrock appears to dip to the south from the road surface to 4 m depth or more under the extracted pit.

5.5. Site 4

The 200 MHz profile collected across Main Street and pit 3, continues southward downslope and terminates just above the MEC where pit 4 (Fig. 2) was excavated (Figs. 3, 4, and 10). The pit was extracted immediately south of a steep (~20°) south-southeast–facing hillside. This hillside, therefore, receives significant solar insolation; however, the pit was extracted on a lower angle (~5°) road cut, likely resulting in lower solar insolation. The pit revealed over 2 m of ice situated below 0.4 m of unfrozen stratified fill and 0.3 m of frozen stratified fill (Fig. 11). For site 4 we used multiple methods to validate depth because the precise location of the pit relative to the GPR transect was unknown

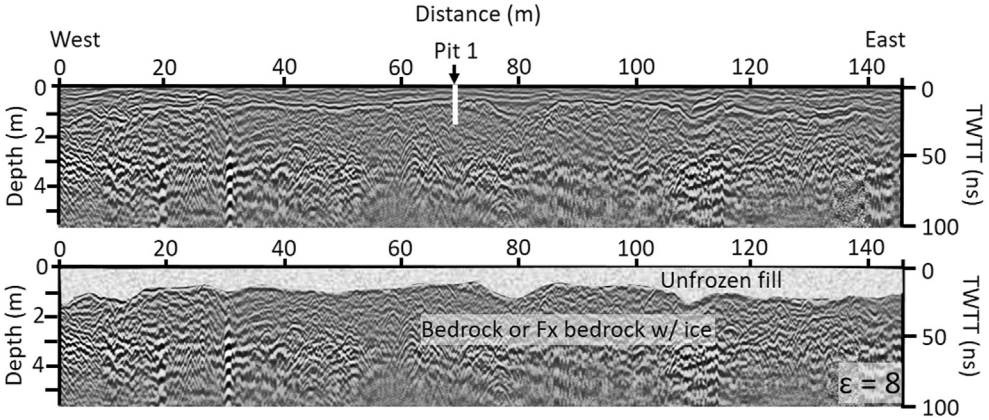

Fig. 6. 200 MHz processed GPR profile (top) showing interpretation of fill and fractured (Fx) rock over ice-rich fractured bedrock (bottom).

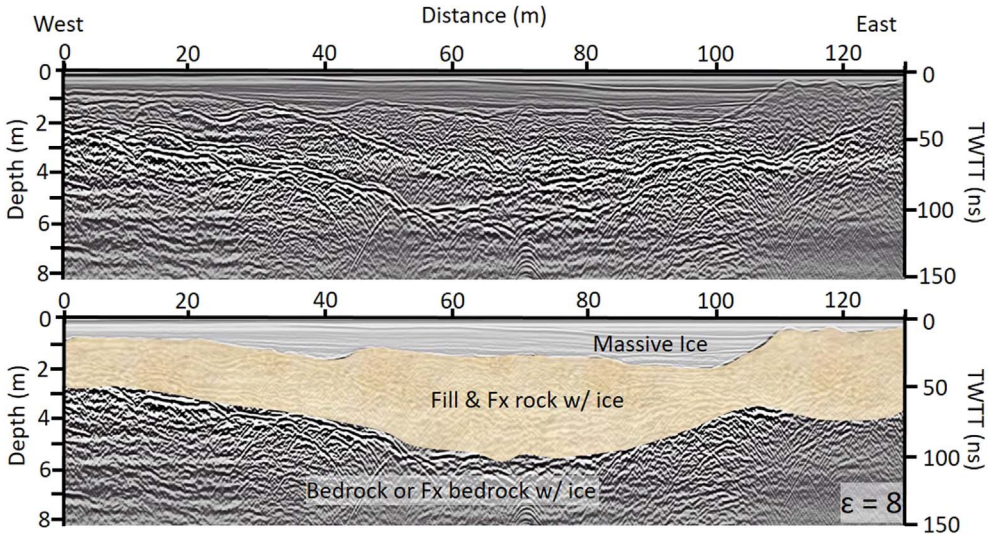

Fig. 7. 200 MHz processed GPR profile (top) between T-Site and Observation Hill oriented parallel to and north of Main Street. Profile is located east of site 1 where a ground-truth pit was extracted. The interpretation (bottom) shows snow and ice over a stratified ice-rich matrix and bedrock at greater depths.

and because the horizon depth to buried ice was quite variable within the pit. Fortunately, several classic hyperbolas existed within the GPR profile, which also had real-time kinematic GPS precision for horizontal geo-referencing within ± 0.1 m. Through migration and calculating a slope of diffraction tails originating near the surface, we determined the top 0.5–0.8 m of fill to be $\acute{\epsilon}$ = 11.4–12.4 with respective wave velocities of 0.089 and 0.085 m ns^{1}, resulting in a 6-cm uncertainty between the two methods when calculating depth to the top of ice (1.55 or 1.49 m, respectively). The ice was assumed to have an $\acute{\epsilon}$ of about 3–4 (e.g. Thomson et al., 2012). We therefore calculated an ice thickness between 2 and 4 m based on a 25–50 ns TWTT. Note that we used our GPR interpretation of this ice to select pit 4 for ground truth. This indicates the utility of GPR for locating and delineating massive ice because it has a very clear boundary and exhibits far less speckle noise and ringing relative to the surrounding near-surface geology.

5.6. Site 5

Site 5 was situated at the southwestern edge of building 155, which is in the central region of the proposed facilities upgrade for McMurdo Station. A pit was excavated in this region to 3 m depth (Fig. 2), and it revealed 0.23 m of fine-grained, thawed, stratified, reddish sands that likely originate from heavily weathered local scoria which were deposited here via construction activities (Affleck et al., 2017). The same fine-grained and stratified sands existed below this point, only frozen, for another 0.36 m. Below these sands, an ice-rich, heavily fractured, and unstratified bedrock fill existed to the bottom of the pit. One worthy note at this location from Affleck et al. (2017) was the strong presence of hydrocarbon odor. Prior studies (Kennicutt II et al., 2010; Klein et al., 2012) mapped petroleum hydrocarbons between 500 and 1000 ppm in this region. A 200 MHz profile collected over this area revealed stratified layers that we interpret as the sand fill noted above within the top 15–20 ns TWTT or 0.79–1.0 m depth where $\acute{\epsilon}$ is assumed to be approximately 8 (Fig. 12). Below this fill, some noted low frequency hyperbolic reflections occur that we assume to be off-axis reflections from local buried debris or building foundations. However, the most note-worthy feature in this profile is a difference in high-frequency speckle noise and signal attenuation between 100 and 180 m distance along the profile, relative to either side of this region. We interpret this region to contain high concentrations of buried

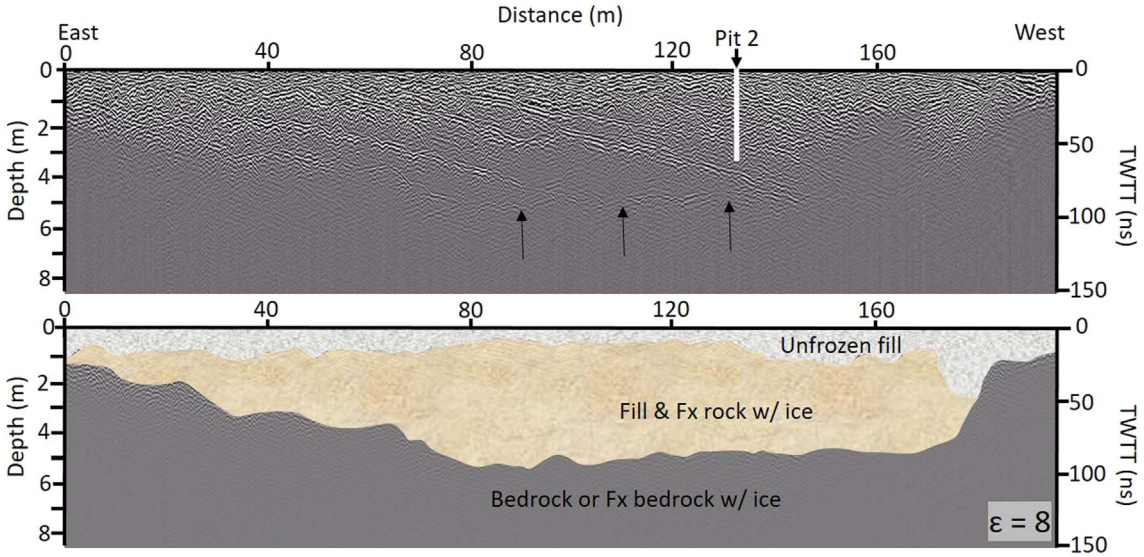

Fig. 8. 200 MHz GPR profile collected across site 2, which was extracted from a raised fill platform. The profile reveals dipping stratified fill with primary horizons likely representing ice lenses within fill deposits. Fill is truncated at depth by a higher $\acute{\epsilon}$ relative to the fill. We interpret this horizon, indicated by black arrows, to represent a transition to solid bedrock.

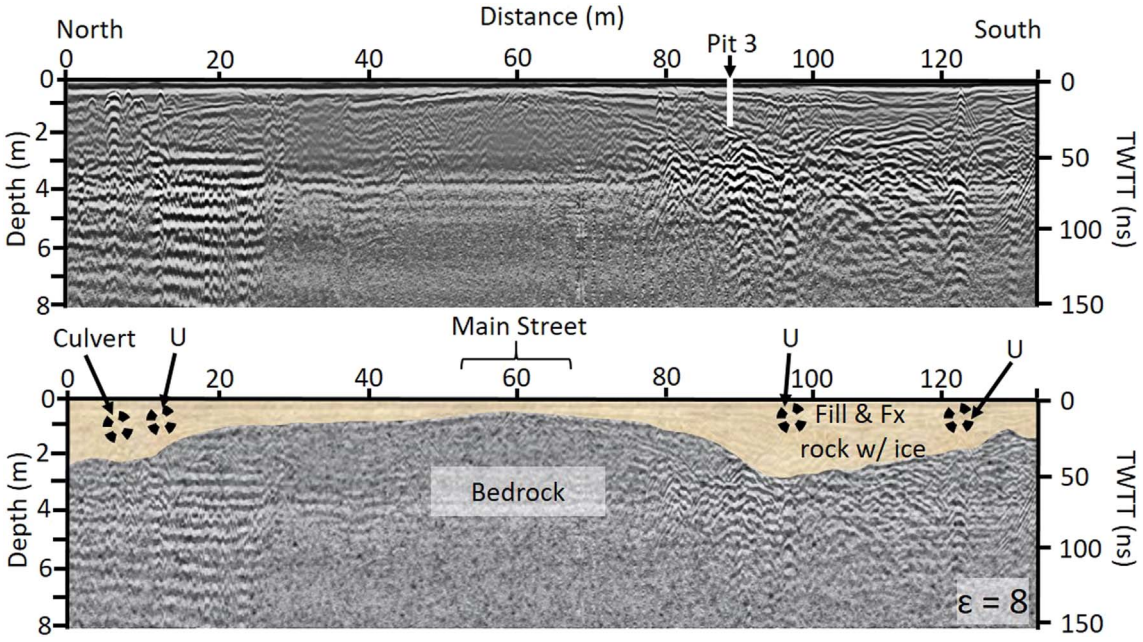

Fig. 9. A 200 MHz profile (top) collected across and perpendicular to Main Street, also crossing a pit extracted from site 3 for ground truth. Our interpretation (bottom) shows bedrock exposed at the surface on Main Street and the bedrock horizon dipping under stratified fill to the north and south. Also note multiple buried utilities (U) to the north and South of Main Street.

hydrocarbons, likely from a spill event. We discuss this in detail below.

6. Discussion

6.1. Bedrock, stratified, and unstratified fill

McMurdo Station is located on terrain that slopes to the south-southwest and is constrained by Observation Hill, Twin Crater, and Arrival Heights to the east, north, and west, respectively (Fig. 1). In general, the station consists of a series of raised stratified sediment platforms placed over a sloping bedrock base to facilitate the construction of facilities or outside storage space. Roadways typically consist of a similar stratified fill to 1–3 m depth over unstratified and heavily fractured bedrock (e.g., Figs. 6 and 9). Depth to bedrock is highly variable, which is consistent with the rough outcrops situated around McMurdo, suggesting a rough, small-scale basin-and-trough structure. The variable thicknesses of anthropogenic fill are dependent on this rough bedrock surface; that is, fill was used to fill depressions between bedrock outcrops. Fill thickness tends to be greater towards the south, suggesting that the region closer to the ocean has been consistently built up or that through natural geomorphological processes fill is washed downhill towards the ocean, therefore creating thicker bedding relative to the upslope region. This interpretation is supported by numerous bedrock outcrops being exposed near T-Site, the dump, and Main Street, but no bedrock outcrops existing near the shoreline to the east and south of Winter Quarters Bay and McMurdo Station, respectively (Fig. 1). The stratified fill is most easily identified by semi-parallel surface conformable horizons or horizons that have been crosscut at the surface due to construction activities following the initial filling effort (e.g., Fig. 8). Boreholes and pits have revealed substantial ice within fill pore spaces and under fill. Personnel who are familiar with McMurdo Station construction activities over the past few

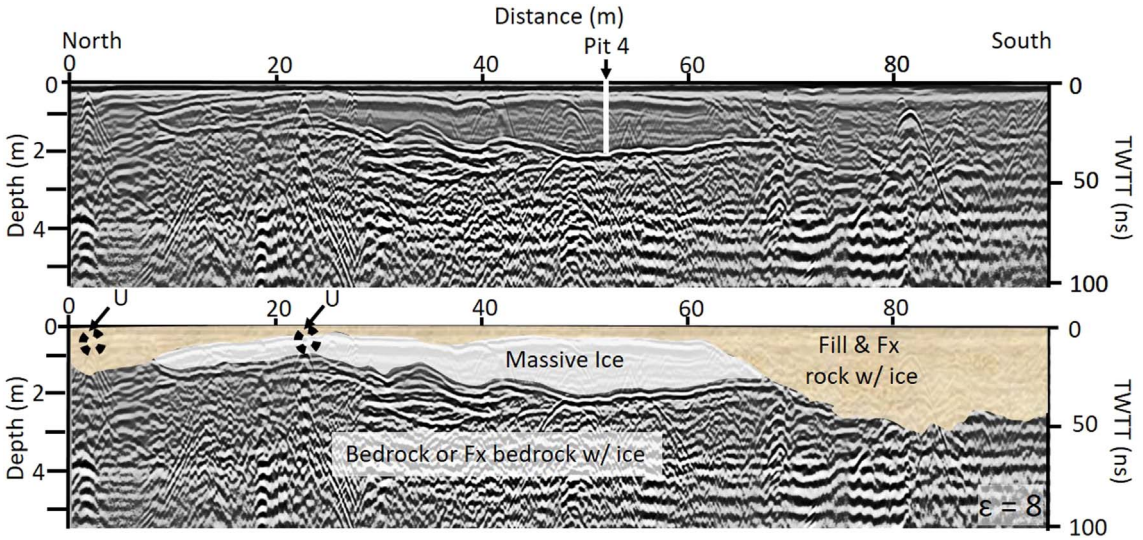

Fig. 10. 200 MHz GPR profile (top) and interpretation (bottom) of the location of site 4 and an extent of massive ice. Note the clear and speckle-free massive ice relative to the surrounding geology and buried utilities (U).

Fig. 11. Photo of the pit 4 showing massive ice buried beneath a shallow cover of stratified thawed and frozen fill.

decades (e.g., Stephen Zellerhoff, U.S. Antarctic Program, personal communication 2015) confirm that many fill platforms have been constructed on solid snow or firn patches, likely resulting in metamorphosed ice under fill. Many dipping stratified horizons also terminate oblique to a rough and semi continuous horizon that is often characterized by a series of diffractions (Figs. 7 and 8). We interpret this horizon to generally represent the solid bedrock contact below the stratified fill based on the unconformity, numerous diffractions, and generally higher relative attenuation below this horizon, which seems consistent with observations of GPR profiles collected over shallow bedrock on and immediately north of Main Street.

6.2. Permafrost, annual freeze, and buried ice

A secondary goal of this study was to locate frozen ground, massive ice, or ice-rich sediments. Results from cores and pits reveal that the stratified fill, unstratified fill, and heavily fractured bedrock across almost all of McMurdo, is ice-rich. This is indicative of summer melt penetrating into the subsurface and refreezing during the long winter months. Some pits and corresponding GPR profiles reveal locations with an active layer situated above perennially-frozen or excess ice-filled sediments greater than 1-m thick (e.g. Figs. 10 and 11). Based on consistent ground-truth and geophysical observations presented above, we can interpret other examples of ice-rich sediments in GPR profiles

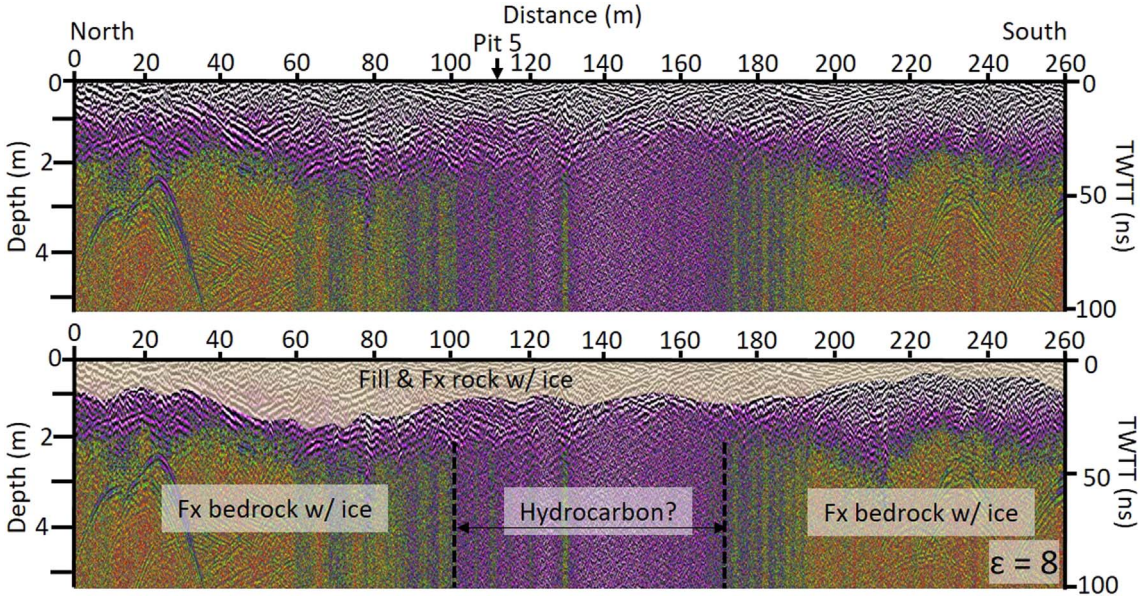

Fig. 12. 200 MHz GPR profile (top) with interpretation (bottom) showing approximate extent of hydrocarbon pollution within the fill and fractured rock, which significantly increases attenuation and noise in the radar signal. Colour scheme represents amplitude of returns with high amplitude returns and scattering being represented by purple. (For interpretation of the references to colour in this figure legend, the reader is referred to the web version of this article.)

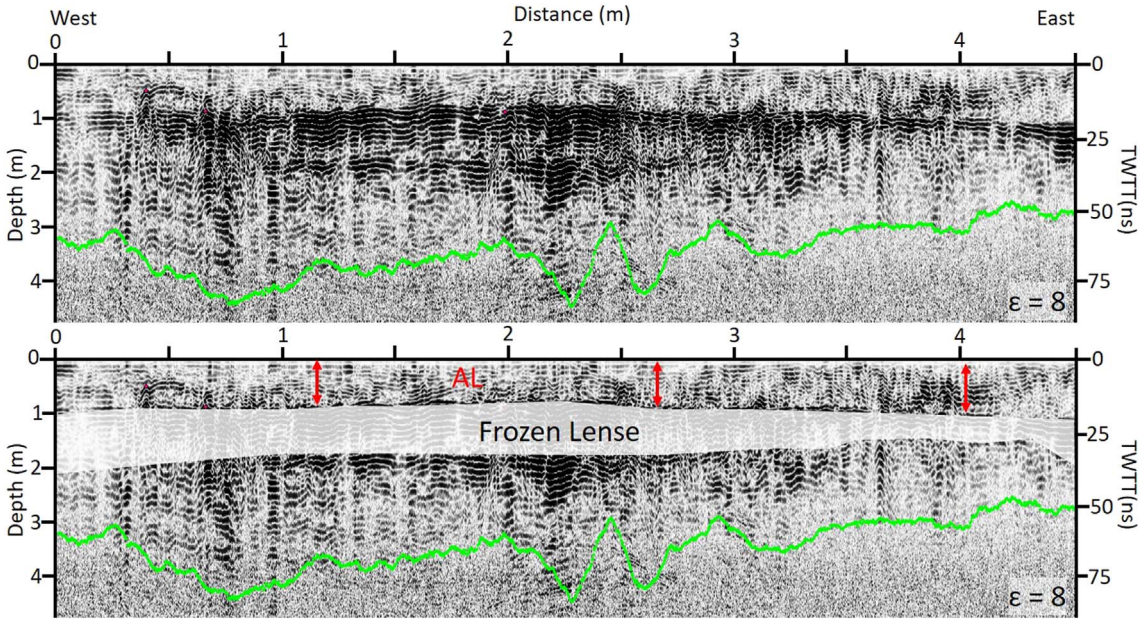

Fig. 13. 400 MHz profile (top) and interpretation (bottom) collected below Crary Lab in January of 2015 showing the active layer above a strong set of parallel and surface-conformable horizons at 1 and 2 m depth, likely representing the top and bottom of a frozen lens. Note that the depth of maximum signal penetration (black line) is likely influenced by water content within the deeper soils and geology.

where no ground-truth was available. For example, in a GPR profile collected down-catchment and to the west of Crary Laboratory in a relatively shaded region, we interpret an active layer over a ~1-m thick frozen lens (Fig. 13). The radar signal is strong through the frozen ground but rapidly attenuates below the lens as in other GPR profiles collected across McMurdo. This example is like the profile collected in November of 2015 below the south-facing hillslope north of the MEC where a nearly 2-m thick massive ice lens existed in the subsurface (Figs. 10 and 11). In both cases, frozen ground likely formed from melt off the neighboring hillslope percolating into the subsurface and re-freezing on an annual basis. Our interpretation of frozen ground below an active layer in Fig. 11 is based on the radar triplet response (Arcone et al., 2003) of the interface, which suggests a higher $\acute{\epsilon}$ above a lower $\acute{\epsilon}$, consistent with thawed fill over frozen fill. Saturated sand and gravel have a $\acute{\epsilon}$ between 10 and 30 (Arcone et al., 2014) whereas frozen ground (i.e., permafrost) typically exhibit $\acute{\epsilon}$ values around 5–8 (Briggs et al., 2016); these values and the moist surface conditions during data collection in January, support our interpretation.

6.3. Quantitative and qualitative assessment of water content

GPR has been used to qualitatively and quantitatively estimate water or ice content within the near surface (Arcone et al., 2014). This could then theoretically be used to infer subsurface drainage patterns. In practice, free water within the subsurface causes high signal attenuation rates and, therefore, quantitative differences in depth of signal penetration relative to areas of the same geology and lower water content. Diffraction analyses, migration, and common midpoint or wide-angle reflection and refraction surveys can be used to estimate pore water content within the subsurface by using radar data if porosity of the matrix material is known. In reality, estimating water or ice content is more difficult because constraints on values of $\acute{\epsilon}$ for the matrix geological material, either bedrock or fill in this case, is rarely available. Complications also arrive because water or ice content can change on short and long-time scales (seasonally to daily) so that ground truth that was not collected concurrent with geophysical data becomes less quantitatively valuable.

In McMurdo, there are regions that may be estimated to have higher or lower water saturation based on the depth of penetration. However, because of variations of thicknesses in road overburden (sand, gravel, etc.) and their associated rates of attenuation, water cannot be considered the sole influence on attenuation. Also, in regions where salt-water infiltration occurs (regions closer to the shore) higher attenuation rates occur because salt is highly conductive. An example of attenuation variability can be found on Hut Point Road, the region north of Winter Harbor shows deeper signal penetration than west of the pier, which is closer to sea level (Fig. 14). We attribute this high attenuation to the salt water table, which likely has infiltrated the sediments alongside the pier. Through further spatial quantitative analysis of GPR depth of penetration (which is the noise floor as displayed in Figs. 13 and 14) relative to the mapped slope and gradient of McMurdo determined from high-resolution LIDAR or other DEM datasets, we may validate GPR as a tool to map sub-surface water flow, a useful analytic for future geotechnical engineering and design at McMurdo Station.

6.4. Hydrocarbon pollution

GPR has proven useful under certain conditions for mapping subsurface hydrocarbon pollution or other chemical spills (e.g., Atekwana et al., 2000; Cameron and Goodman, 1989; Daniels et al., 1995; Lopes de Castro and Branco, 2003), particularly when prior profiles were collected at a site for comparison to the region after a spill. Buried hydrocarbons or other light non-aqueous phase liquids (such as gasoline, diesels and other petroleum products) result in higher local attenuation rates and speckle noise in GPR profiles relative to the surrounding region. Similar effects can occur from pore spaces filled with water; however, both hydrocarbons and water signatures are distinct from buried debris or general attenuation from the matrix material because buried debris is often point specific, resulting in diffractions, and general attenuation should be relatively consistent spatially when surveying over the same geological material. Near the center of McMurdo Station, we show a case example of likely hydrocarbon contamination (Fig. 12) based on the speckle noise and attenuation of the location relative to the surrounding region. Pit 5 extracted at this site (Figs. 3 and 4; Pit 5) also revealed significant hydrocarbon levels within the sediments. High hydrocarbon concentrations were also noted by other studies for this region (Kennicutt II et al., 2010; Klein et al., 2012). Both findings support our interpretation; however, our

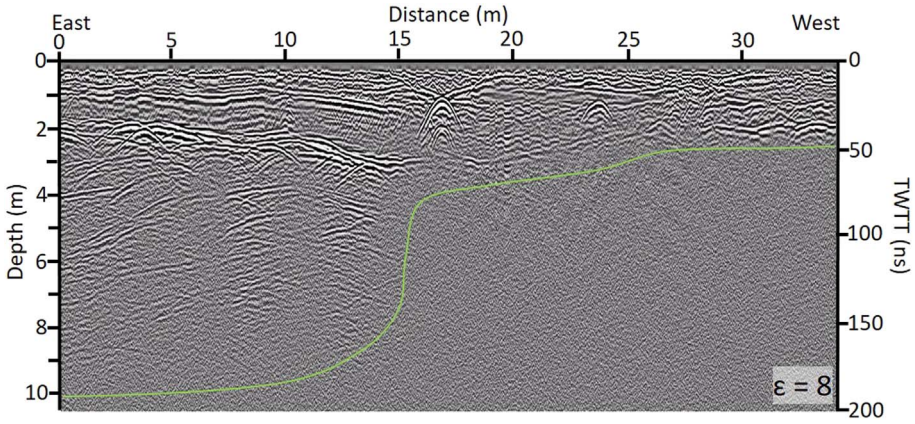

Fig. 14. 200 MHz profile collected down Hut Point Road towards Discovery Hut showing a significant change in depth of radar signal penetration at 15 m distance (black line) due to higher attenuation rates from saltwater intrusion.

interpretation should be combined with more detailed chemical and physical analysis of borehole data to definitively confirm this finding and to estimate the total spatial extent of the spill if it does in fact exist.

6.5. Utilities

Utilities are readily visible within most radar datasets. At McMurdo, the 200 and 400 MHz antennas both imaged buried utilities at 0.3–8 m in depth (e.g., Figs. 9 and 10). Utilities are typically imaged by GPR as finite hyperbolic reflectors with the apex of each reflection providing an estimate of where the GPR antenna crossed the center of a utility line. The slope of the hyperbolic diffraction tail is a function of the angle of approach relative to the orientation of the utility line and the radio wave velocity as it travels within the geological medium above and surrounding the utility. A classic response from electrical utilities is ringing of hyperbola to greater depths under the most-shallow hyperbola (e.g., Figs. 9 and 10). Other objects can cause similar reflections, such as buried debris, within the surrounding geological matrix (e.g., stones, or old construction debris). Interpretation of the triplet response typically resolves any ambiguity in the cause of these hyperbolas due to metallic objects having an $\acute{\epsilon}$ assumed to approach infinity (∞).

7. Limitations of GPR

GPR is an excellent tool for rapid near-surface and nondestructive assessment of local geology and for geotechnical purposes such as those outlined here. However, some challenges exist that limit its efficacy or that must be considered when interpreting results. Radar signals are significantly attenuated by certain materials, such as metals and salt water (both highly conductive) and magnetic rocks. High free (pore) water content within a geological medium also significantly attenuates signals. In contrast, resistive materials, such as dry permafrost, ice, snow, firn, sand, and gravel, provide a good medium to propagate electromagnetic waves. Sources of noise include poor ground coupling or interference from radios or local transmitters nearby that transmit on similar frequencies. Poor ground coupling causes loss of energy at the surface and usually occurs when the terrain is rough or irregular. Rough terrain includes boulder-strewn surfaces and pothole or washboard-covered gravel roads, whereas snow cover (common in the early season) provides good ground coupling and less associated energy loss at the surface. Radio interference is usually of greatest concern in urban areas; however, any location that relies heavily on radio transmissions can negatively impact GPR data if center frequencies overlap because bandpass filtering is no longer an option.

A comparison of data collected in McMurdo during the early (October–November) and late (January–February) seasons revealed significantly higher noise and attenuation during the late season. We attribute the poor quality of data collected during the spring to a lack of snow cover (which caused bouncing of the antenna across uneven terrain and associated poor ground coupling) and meltwater within the subsurface. We therefore suggest that future McMurdo surveys should be conducted during the early season to minimize attenuation and to improve ground coupling. However, if the primary goal is to image the active layer and locate massive ice within the near surface, mid-season studies are appropriate because a strong contrast exists between the thawed active layer and frozen material below. Certain materials, such as some basalts and silt, also have inherent high attenuation rates; this issue cannot be mitigated within this case study. Radio transmission interference and highly conductive metal reflectors (e.g., culverts, buildings and foundations, and buried utilities) limit GPR applications in many locations. For example, the transmissions of radio signals by McMurdo operations can cause noise between certain frequencies. Also, syncing the GPR system with an RTK GPS system to improve spatial accuracy worked for the 200 MHz dataset; however, the RTK system transmitted at 418 MHz. This resulted in significant noise within the 400 MHz dataset. Because of the similarity in frequencies, we were unable to filter the RTK noise from the 400 MHz GPR data. Hence, we opted to not use the RTK system with that antenna, which resulted in about a 1–3 m spatial accuracy as opposed to the roughly 0.25 m accuracy of the 200 MHz data, which was collected with RTK GPS.

8. Conclusions

In this study, we distinguish between stratified anthropogenic fill, unstratified or heavily fractured fill, and bedrock by using a variety of assumptions in conjunction with ground truth via geological cores and excavated pits. Variability of $\acute{\epsilon}$ from 6 to 12 across McMurdo Station results in depth uncertainties of 1-m or more, particularly in areas where ground truth is nonexistent. This is particularly true for deeply buried bedrock. More fill exists in the southwest region of McMurdo Station near the shoreline whereas bedrock outcrops in northeast McMurdo are numerous, providing good ground truth for extrapolation of GPR profiles. Much of the stratified and unstratified fill or heavily fractured bedrock is ice-rich throughout McMurdo, according to cores and pits; this is generally confirmed with GPR profiles.

Seasonality of data collection dictated penetration success, as did local activities such as dust suppression efforts. For example, late-season data collection (January–February) resulted in water-rich surface soils that created more noise and higher attenuation rates in radar profiles. Application of salt water on road surfaces as a dust suppression tool also significantly attenuated radar signals in the spring. In contrast, depth of penetration was greatly increased and noise was reduced during early season (November) when minimal melting had yet occurred. Of the antennas used, the 100 MHz was noisy and virtually unusable in this environment, and the 400 MHz had less noise but also

reached minimal depths of penetration (1–2 m). The 200 MHz antenna was a reasonable compromise because it could image relatively deep (5–10 m) yet also provided reasonable vertical resolution of near-surface structures. The antenna also resulted in the least noise of the three antennas used. All three commercial antennas used are shielded, however, results show that they were still not impervious to environmental noise, particularly around the given frequencies of each antenna.

This study established several recommendations that may improve the efficacy and benefits of GPR at McMurdo Station or at other similar sites situated in cold regions. First, to improve ground coupling, minimize attenuation, and maximize depth of penetration, data collection should occur during the early season when snow covers much of the ground and minimal meltwater exists within the fill. Caveats to this recommendation exist, however. If assessment of the active-layer thickness variability is of interest, then a late season data collection should occur. Also, if salt is applied to the road at any time, attenuation rates increase significantly. Subsurface conditions vary significantly temporally and spatially depending on slope, aspect, summer and winter temperatures, and snow cover.

Vast quantities of data can be collected over this terrain; however, without adequate ground truth, numerous assumptions are required to quantify geophysical results into water–ice content, attenuation rate of materials, and depth to various horizons, such as bedrock. Therefore, to better constrain geophysical results, we recommend that future studies in such a complex area, focus on providing ground truth at specific locations of interest that correspond with known continuous horizons or diffractions within GPR profiles. It is likely that with this design, quantitative data analysis of GPR profiles could include quantification of radar signal attenuation that could be used to determine subsurface water flow pathways and transitions between near-surface geological structures (till or bedrock) with greater certainty.

Funding

This work was for the National Science Foundation (NSF) and was supported under the award number #1564557, U.S. Army Cold Regions Research and Engineering Laboratory for support to the United States Antarctic Program (USAP), Engineering for Polar Operations, Logistics, and Research. Funding was also provided by the University of Washington, Future of Ice Program.

References

Affleck, R.T., Campbell, S., Sinclair, S., Tischbein, B., 2017. Subsurface Assessment at McMurdo Station, Antarctica. ERDC/CRREL TR-17-4. U.S. Army Engineer Research and Development Center, Hanover, NH.

Affleck, R., Carr, M., 2015. Predicting when peak discharge occurs for ephemeral flow at McMurdo Station watershed. In: Proc. 2015 International Conference on Cold Regions Engineering: Developing and Maintaining Resilient Infrastructure, 19–22 July 2015, Salt Lake City, Utah.

Affleck, R.T., Carr, M., Elliot, L., Chan, C., Knuth, M., 2014a. Pollutant Concentration in Runoff at McMurdo Station, Antarctica. ERDC/CRREL TR-14-15. U.S. Army Engineer Research and Development Center, Hanover, NH.

Affleck, R.T., Carr, M., Knuth, M., Elliot, L., Chan, C., Diamond, M., 2014b. Runoff Characterization and Variations at McMurdo Station, Antarctica. ERDC/CRREL TR-14-6. U.S. Army Engineer Research and Development Center, Hanover, NH.

Affleck, R., Carr, M., West, B., 2014c. Flow Control and Design Assessment for Drainage System at McMurdo Station, Antarctica. ERDC/CRREL TR-14-26. U.S. Army Engineer Research and Development Center, Hanover, NH.

Affleck, R., Vuyovich, C., Knuth, M., Daly, S., 2012. Drainage Assessment and Flow Monitoring at McMurdo Station During Austral Summer. ERDC/CRREL TR-12-3. U.S. Army Engineer Research and Development Center, Hanover, NH.

Arcone, S.A., Campbell, S., Pfeffer, W.T., 2014. GPR profiles of glacial till and its transition to bedrock: interpretation of water content, depth and signal loss from diffractions. Journal of Engineering and Environmental Geophysics 19 (4), 207–228. http://dx.doi.org/10.2113/JEEG19.4.207.

Arcone, S.A., Peapples, P.R., Liu, L., 2003. Propagation of a ground-penetrating radar (GPR) pulse in a thin-surface waveguide. 68 (6), 1922–1933.

Atekwana, E.A., Sauck, W.A., Werkema, D.D., 2000. Investigations of geoelectrical signatures at a hydrocarbon contaminated site. J. Appl. Geophys. 44 (2–3), 167–180. http://dx.doi.org/10.1016/S0926-9851(98)00033-0.

Briggs, M.A., Campbell, S., Nolan, J., Walvoord, M.A., Ntarlagiannis, D., Day-Lewis, F.D., Lane, J.W., 2016. Surface geophysical methods for characterising frozen ground in transitional permafrost landscapes. Permafr. Periglac. Process.(April 2015). http://dx.doi.org/10.1002/ppp.1893. (n/a-n/a).

Cameron, R.M., Goodman, K.S., 1989. Detection and Mapping of Subsurface Hydrocarbons with Airborne Ground-Penetrating Radar. Proc. 3rd Nati Outdoor Action Conf, Orlando, Fla.

Campbell, I.B., Claridge, G.G.C., Balks, M.R., 1994. The effect of human activities on moisture content of soils and underlying permafrost from McMurdo Sound region, Antarctica. Antarct. Sci. 6 (3), 307–314.

Cole, J.W., Kyle, P.R., Neall, V.E., 1971. Contributions to quaternary geology of Cape Crozier, White Island and Hut Point Peninsula, McMurdo Sound region, Antarctica. N. Z. J. Geol. Geophys. 14 (3), 528–546. http://dx.doi.org/10.1080/00288306.1971.10421946.

Crockett, A.B., 1998. Background levels of metals in soils, McMurdo Station, Antarctica. Environ. Monit. Assess. 50, 289–296.

Daniels, J.J., Roberts, R., Vendl, M., 1995. Ground penetrating radar for the detection of liquid contaminants. J. Appl. Geophys. 33 (1–3), 195–207. http://dx.doi.org/10.1016/0926-9851(95)90041-1.

Elshafie, A., Heggy, E., 2012. Dielectric properties of volcanic material and their role for assessing rock. 43rd Lunar and Planetary Sciences Conference 43, 43–44.

Elshafie, A., Heggy, E., 2013. Dielectric and hardness measurements of planetary analog rocks in support of in-situ subsurface sampling. Planet. Space Sci. 86, 150–154. http://dx.doi.org/10.1016/j.pss.2013.02.003.

Fenwick, J., Winkler, D., 2016. Geotechnical Assessment Report: McMurdo Station. Ross Island, Antarctica.

Kennicutt II, M.C., Klein, A., Montagna, P., Sweet, S., Wade, T., Palmer, T., ... Denoux, G., 2010. Temporal and spatial patterns of anthropogenic disturbance at McMurdo Station, Antarctica. Environ. Res. Lett. 5 (3), 1–10. http://dx.doi.org/10.1088/1748-9326/5/3/034010.

Klein, A.G., Kennicutt, M.C., Wolff, G.A., Sweet, S.T., Bloxom, T., Gielstra, D.A., Cleckley, M., 2008a. The historical development of McMurdo station, Antarctica, an environmental perspective. Polar Geogr. 31 (3–4), 119–144. http://dx.doi.org/10.1080/10889370802579856.

Klein, A.G., Kennicutt, M.C., Wolff, G.A., Sweet, S.T., Gielstra, D.A., Bloxom, T., 2008b. Disruption of sand-wedge polygons at McMurdo Station, Antarctica: an indication of physical disturbance. In: Proceeding of the 61st Eastern Snow Conference, Portland, ME.

Klein, A.G., Sweet, S.T., Wade, T.L., Sericano, J.L., Kennicutt, M.C., 2012. Spatial patterns of total petroleum hydrocarbons in the terrestrial environment at McMurdo Station, Antarctica. Antarct. Sci. 24 (5), 450–466. http://dx.doi.org/10.1017/S0954102012000429.

Kyle, P.R., Muncy, H.L., 1989. Geology and geochronology of McMurdo volcanic group rock in the vicinity of Lake Morning, McMurdo Sound, Antarctica. Antarct. Sci. 1 (July), 345–350.

Lopes de Castro, D., Branco, R.M.G.C., 2003. 4-D ground penetrating radar monitoring of a hydrocarbon leakage site in Fortaleza (Brazil) during its remediation process: a case history. J. Appl. Geophys. 54 (1–2), 127–144. http://dx.doi.org/10.1016/j.jappgeo.2003.08.021.

Rust, A.C., Russell, J.K., Knight, R.J., 1999. Dielectric constant as a predictor of porosity in dry volcanic rocks. J. Volcanol. Geotherm. Res. 91 (1–2), 79–96. http://dx.doi.org/10.1016/S0377-0273(99)00055-4.

Sullivan, W., 1957. Quest for a Continent. McGraw-Hill, New York, New York.

Thomson, L.I., Osinski, G.R., Pollard, W.H., 2012. The Dielectric Permittivity of Terrestrial Ground Ice Formations: Considerations for Planetary Exploration Using Ground-Penetrating Radar.

Wright, A.C., Kyle, P.R., McIntosh, W.C., Klich, I., 1982. Geological field investigations of volcanic rocks at Mount Discovery and Mason Spur, McMurdo Sound seismic reflection profiling in McMurdo Sound, 1983-1984. Antarct. J. US 82–83.